Nanowire embedded micro-drilled dual channel approach to develop highly sensitive biosensor

A. K. Pathak, *Senior Member IEEE*, B. M. A. Rahman, *Life Fellow IEEE*, C. Viphavakit, *Senior Member IEEE*

***Abstract*— In this letter, we propose a novel approach to develop a highly sensitive surface plasmon resonance (SPR) based fiber optics biosensor. The sensor comprises a dual-drilled channel (DDC) with gold-nanowire (AuNW) contained in each channel to excite the plasmon modes. The SPR effect between the core guided mode and the surface plasmon polariton (SPP) modes of the DDC is used to evaluate the sensing response with respect to different analytes. The sensing performance, coupling characteristics, and the fabrication tolerance of the sensor are numerically analyzed and characterized by using a full-vectorial Finite Element Method (FEM). The designed sensor shows a minimum sensitivity of 3150 nm/RIU for refractive index (*RI*) = 1.310. While, the sensor exhibits an extremely high sensitivity varying from 10250 nm/RIU to 90500 nm/RIU for RI varied over the range of 1.370 to 1.400. Various structural parameters, e.g., separation of the channel from the core, the radius of the AuNW, the fabrication tolerance, etc., have been studied in this work. In addition, the possible fabrication steps of such a design have been discussed indicating its simple practical realization.**

***Index Terms*— Surface plasmon resonance, biosensor, drilled channel, nanowire, sensor**

I. Introduction

Over the past decades, SPR based sensors have played an important role in various physical and chemical sensing applications [1]. These sensors work on the basic principle of excitation of the surface plasmon waves at the metal-dielectric interface. The SPR technology has attracted researchers for many years due to its high sensitivity, simple structure, rapid response toward the change in the surrounding medium, and label-free detection mechanism. Most of the commercially available SPR sensors are based on Kretschmann or Otto configurations [2], [3]. The first SPR based sensing configuration was reported by Liedberg *et al.* for gas and biosensing [4], which although, performed effectively, but main limitations were its bulky size and mechanical instability. These shortcomings can be avoided by using fiber-based sensing configurations utilizing the SPRs. Optical fiber-based sensors have additional advantages over the prism-based approach, such as their portability, cost-effectiveness, high sensitivity, *in-situ* detection, and immunity to electromagnetic interference.

In most SPR based sensors, some metallic film such as gold, silver, copper, etc. is deposited on the surface of the fiber. However, in 2014, Xiaodong *et al.* proposed a microfiber sensor covered with nanoscale CrNi wire and achieved an enhanced sensitivity of 220.65 nm/A^2 [5]. The role of nanowire in sensing enhancement has been explored over the past decades and the technology progressed further to make the sensing structure simpler and more reliable. In 2019, Fu *et al.* proposed to use polished fiber along with a graphene layer containing a silver nanocolumn for refractive index sensing and achieved a maximum sensitivity of 8860 nm/RIU [6]. Recently, in order to provide a simple structure, Santos *et al.* reported a suspended core optical fiber structure incorporating gold nanowire and achieved good sensitivity in comparison to the conventional single-mode fiber (SMF) [7]. In the same year, we have reported hollow core fiber (HCF) sensor consists of an AuNW and achieve an average sensitivity of 10560 nm/RIU for *RI* = 1.46-1.48 [8]. The major limitation of our previously reported sensor was the difficulty of maintaining fundamental light in large diameter of HCF (40 μm), and its application for high refractive index analyte which is beyond the reported biofluids. Additionally, the reported HCF configuration was a type of microstructured fiber which required filling of measurand for detection like the photonic crystal fibers, which is a complex task itself.

In order to reduce the complexity and maintain the fundamental light, a dual drilled channels (DDC) sensing configuration using commercially available single mode fiber (SMF), is proposed in this letter. The analysis and sensing response of the DDC sensor is performed using a wavelength interrogation technique which utilizes the modal loss analysis in the structural parameter optimization. The numerically simulated results exhibit that the proposed sensor achieves an extremely high sensitivity of 90500 nm/RIU for higher refractive index. To the best of our knowledge, the proposed sensor achieves the highest sensitivity compared to other sensors based on similar techniques [8]–[11]. In addition, the micro-drilling method [12] with the Q-switch laser provides a simple fabrication step and also allows the optical fiber sensor to have precise dimensions compared to that made by using a D-shaped polishing technique [13].

II. Structural Design and Fabrication

The proposed DDC sensor can be easily fabricated using micro-drilling technology [12]. The schematic diagram of the basic steps required to produce such a specialized sensing device is illustrated in Fig. 1. At first, two AuNWs will be synthesized using a traditional ultrasonic-assisted seed-mediated growth method [14] and placed inside two pre-functionalized capillary tubes to ensure adhesion between the nanowire and the capillary. These tubes are later placed at an optimum distance from a Ge-doped solid silica rod and covered with another comparatively large fused silica tube. The main concept of this stack-and-draw technique is to prepare a macroscopic element

This paragraph of the first footnote will contain the date on which you submitted your paper for review. This work is supported by the Second Century Fund (C2F), Chulalongkorn University, and Rachadapisek Sompote Fund for Intelligent Control Automation of Process Systems Research Unit, Chulalongkorn University.

Corresponding author: C. Viphavakit (e-mail: charusluk.v@chula.ac.th).

A. K. Pathak and **C. Viphavakit** are associated with international school of Engineering, Chulalongkorn University, Thailand. (e-mail: akhilesh.k@chula.ac.th, charusluk.v@chula.ac.th)

B. M. A. Rahman is associated with School of Mathematics, Computer Science and Engineering, City University of London, London EC1V 0HB, U.K (email: B.M.A.Rahman@city.ac.uk)

of desired fiber by stacking the whole assembly i.e., AuNWs, capillary tube, glass-rod (core), and large capillary (cladding) according to the optimized design which is also known as a preform. The fabricated preform can then be heated and drawn into microstructured integrated rods and finally pulled into optical fibers [15]. After that, the fabricated fiber is passed through the micro-drilling technique to make dual channels in the fiber. The procedure requires the drilling of a micro-hole dual-channel SMF using a Q-switched Nd: YAG laser to precisely drill the fiber with an optical system that focuses the beam onto a small spot. The same system is also used to visualize the drilling process in real-time with a CCD camera [12]. The drilling technology is more convenient compared to the polishing technology to reach the precise depth for light mater interaction [13]. For the detection, the sensor will be submerged in the analytes of various refractive indices instead of filling measurand in the channel, like photonic crystal fibers.

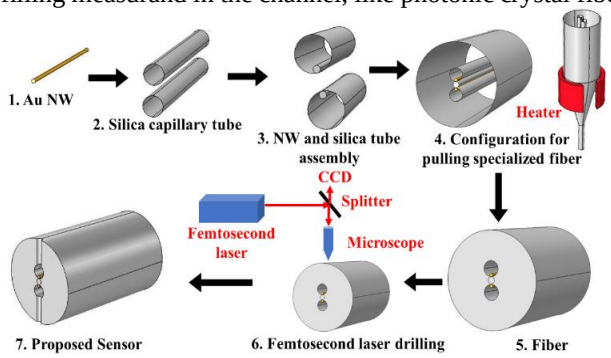

Fig.1. Schematic diagram of the possible fabrication step.

The cross-sectional image of the DDC-assisted Au nanowires (AuNWs) is illustrated in Fig. 2. The DDC has been designed to fit into a standard SMF for the maximum coupling of light with the measurand and AuNWs. The proposed sensor is designed on a SMF, by considering its core/cladding diameter to be 9/125 µm, capillary size (*S*) 10 µm, and drilling width (*W*) 5 µm. Here, the separation of DDC (*D*) from the core and the radius of AuNWs (r_n) are optimized before characterizing the whole configuration as a sensor. In the proposed work, the analyses have been performed using a 2D modal simulation. The FEM is used to conduct all numerical analyses, in order to study the electromagnetic polarization (EP) feature of the SPR mode and the core mode.

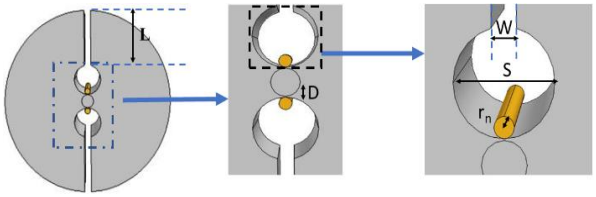

Fig. 2. Cross-sectional view of the proposed sensor design.

The refractive index (*RI)* of the silica fiber materials is obtained from the Sellmeier relation [15]. The dielectric constant of AuNWs is evaluated using the Lorentz-Drude model [16].

$$\varepsilon_m = 1 - \frac{\Omega_p^2}{\omega(\omega - j\Gamma_0)} - \sum_{j=1}^{k} \frac{f_j \omega_p^2}{(\omega_j^2 - \omega^2) + j\omega\Gamma_i} \qquad (1)$$

where, ε_m, ω, Ω_p, and Γ_0 represent the dielectric constant, angular frequency, plasma frequency, and damping frequency, respectively. In this equation, $\Omega_p/2\pi$ = 2113.6 THz and $\Gamma_0/2\pi$ = 15.92 THz. The spectral width and frequency of the Lorentz oscillator are denoted by Γ_i and ω_p, respectively. In addition, $\omega_p/2\pi$ = 650.07 THz and $\Gamma_i/2\pi$ = 104.86 THz [16].

III. RESULTS AND DISCUSSION

The excitation of SPR can be characterized by calculating the modal loss of the guided mode, which is the key parameter for every SPR based fiber sensor. The modal loss of the proposed DDC is evaluated from the imaginary part of the effective refractive index ($Im(n_{eff})$). The $Im(n_{eff})$ is directly proportional to the modal loss as shown in the following relation [17]

$$\alpha\left(\frac{dB}{m}\right) = 8.686.k_0 Im(n_{eff}) \qquad (2)$$

where k_0 is the vacuum wavenumber ($k_0 = 2\pi/\lambda$).

Figure 3 illustrates the dispersion affinity of the SPR and core modes, along with the corresponding spectral loss with the wavelength for the optimized parameter of sensor i.e., D = 0.2 µm, r_n = 0.5 µm, S = 10 µm, W = 5 µm, and RI = 1.33. It can be observed that the n_{eff} of the core guided mode varies almost linearly as shown by the black dots. However, as the operating wavelength increases, the SPR mode reduces (shown by the red dots) gradually and intersects with SPR at λ = 1.108 µm for RI = 1.330, which is known as the resonance wavelength (λ_R). The intersection phenomena of both n_{eff} takes place where the maximum power from the core mode transfers to the plasmonics modes and gives the maximum loss (shown by the blue line). As a result, the peak can be seen at the point of intersection which is also at λ = 1.108 µm in Fig. 3. A sudden shift of n_{eff} from core mode to SPR mode can be observed at the resonance wavelength, due to the sudden energy exchange between the two modes.

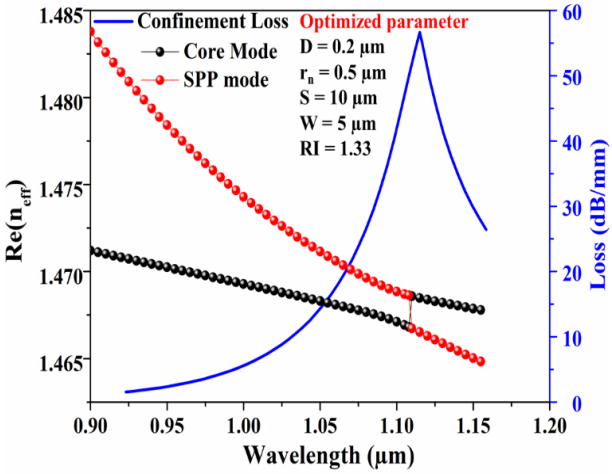

Fig..3. Dispersion curve of the proposed sensor for core and SPR modes at *RI* =1.33.

Figures 4(a), (b), and (c) illustrate the field distributions of the fundamental mode, SPR mode, and the phase-matched mode, respectively. As we can see in Fig.4 (a), the maximum light is confined within the core region at λ = 0.9 µm. On the other hand, Fig. 4(b) shows the SPR mode where the maximum energy has been transferred to the AuNWs region. However, Fig. 4 (c) shows the phase-matched coupled supermodes between the fundamental mode and SPR mode when the n_{eff} of both isolated modes become almost similar. This is defined as the resonance condition. At this resonant wavelength (λ_R) the energy gets completely transferred from the fundamental core mode to the plasmonic mode and forms supermodes which reach the maximum loss of 56.66 dB/mm.

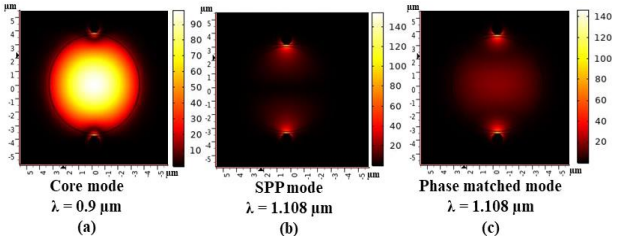

Fig.4. Field distribution in (a) fundamental mode, (b) SPR mode, and (c) phase-matched mode.

The optimization of all of the structural parameters such as the nanowire radius, the separation of DDC, and the size of the channel are required to attain the maximum sensing response. The separation of DDC (*D*) from the core of the fiber plays an important role for coupling the light from the core mode to a SPR mode. For the optimization of *D*, the separation is varied from 0.1 μm to 0.5 μm. The highest maximum loss of 56.66 dB/mm is obtained at λ_R = 1.108 μm for *D* = 0.2 μm. With a separation of 0.1 μm, 0.3 μm, 0.4 μm, and 0.5 μm the maximum loss of 48.45 dB/mm, 49.35 dB/mm, 26.63 dB/mm and 17.35 dB/mm are obtained, respectively. The spectral loss for separation *D* is illustrated in Fig.5. A dielectric mode of a fiber is essentially loss less. On the other hand, a plasmonic mode is highy lossy. When a dielectric mode is phase matched to a plasmonic mode, then a coupled supermode can be formed with a very sensitive loss peak. The peak of the spectrum, known as the SPR peak, indicates the maximum energy transfer from the fundamental dielectric mode to a plasmonic mode, which enhances the light interaction to the sensing analytes allowing better sensitivity. Therefore, a sensor is designed to identify the maximum shift of the resonant wavelength of a sharp loss-peak which may happen due to any perturbation of the sensing media and thus to achieve the maximum sensitivity possible. From Fig.5, *D* = 0.2 μm is considered as the optimum separation distance of both channels from the core.

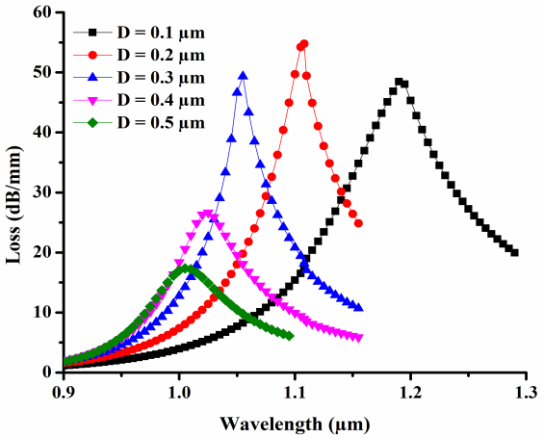

Fig.5. Confinement modal loss spectra with the variation of MFC distance.

The radius of AuNWs (r_n) is varied next by fixing the separation (*D*) at 0.2 μm to achieve the maximum energy for the SPR mode at λ = 1.108 μm. The spectral loss of the core mode with respect to the variation of r_n is shown in Fig. 6. The optimization process takes place at three different radii varying from 0.4 μm to 0.7 μm. It is observed from Fig. 6 that r_n = 0.5 μm exhibits a maximum spectral loss of 56.66 dB/mm at λ_R = 1.108 μm, while r_n = 0.4 μm, 0.6 μm, and 0.7 μm, exhibit a maximum loss of 56.20 dB/mm, 55.92 dB/mm, and 53.51 dB/mm at λ_R = 1.165 μm, 1.068 μm, and 1.030 μm, respectively. Hence, the r_n with a maximum loss for r_n = 0.5 μm at λ_R = 1.108 μm, has been considered as the optimized size of AuNWs in both channels.

Next, the effect of variation of the other sensor parameters are studied. However, as the sensor performance did not vary much with the channel width (*S*) and drilled opening (*W*), these are not shown here. The effects of r_n, on the sensor performance are shown in Fig. 6 when channel width (*S*) and drilled opening (*W*) are taken as 10 μm and 5 μm, respectively.

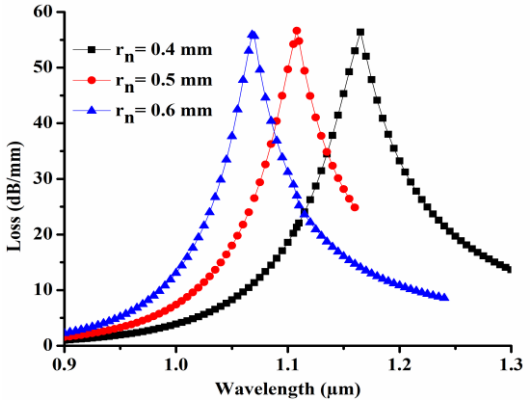

Fig. 6. Confinement modal loss spectra with the variation of nanowire radii.

After attaining the optimized structure, the sensing response of the designed sensor has been investigated for a wide range of analytes varying from *RI* = 1.310-1.400. The variation in the spectral loss as a function of wavelength for different analytes is illustrated in Fig. 7. Figure 7 depicts a good redshift in spectral loss varying from λ_R = 1.035 μm to 2.025 μm. It can be observed that as the *RI* is increased from 1.310 to 1.400, the full width and half maximum (FWHM) of the resonance peaks are broadened. The broadening of these spectra may arise with the *RI* because of the comparative lower refractive index contrast between the core and *RI* solutions causing stronger coupling for weaker confinement of the core mode.

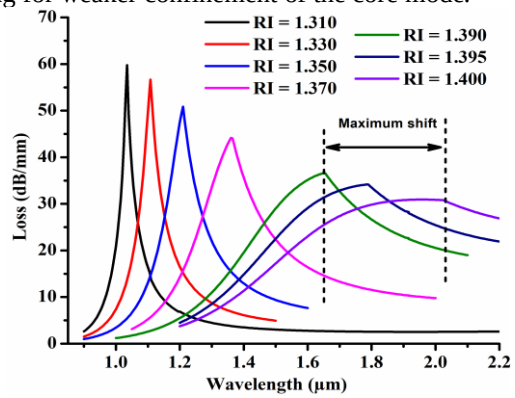

Fig.7. Confinement modal loss spectra with various *RI*.

The maximum peak values of the spectra in Fig. 7 are considered to be the resonance wavelength for different *RI* solutions. Figure 8 illustrates this variation in the resonance wavelength and the sensitivity corresponding to the range of *RI*. From this relationship, a nonlinear variation in resonance wavelength can be seen. To calculate the sensitivity from Fig. 8, the central difference has been determined to estimate the sensitivity of the sensor corresponding to *RI*. Therefore, the sensitivity of the sensor (S_λ) can be calculated from the change in peak λ_R divided by the change in *RI*, as illustrated in the following relation [17]

$$S_\lambda = \Delta\lambda_{peak}/\Delta RI(nm/RIU) \qquad (3)$$

where, $\Delta\lambda_{peak}$ and ΔRI denote the change in the peak of λ_R and the change in the *RI* of the measurand, respectively. The highest sensitivity is achieved for the higher RI range varying between 1.370 and 1.400

due to the maximum energy of propagated light at the interface between the core and the *RI* solutions. The sensitivity corresponding to the RI range is shown in Table.1.

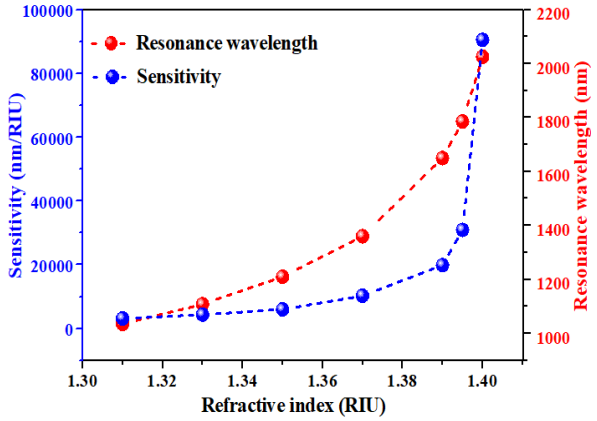

Fig. 8. Variations of the resonance wavelength and corresponding sensitivity with the *RI.*

TABLE.1. RI range and its corresponding average sensitivity

RI	Resonance wavelength (nm)	Sensitivity (nm/RIU)
1.310	1035	3150
1.330	1108	4350
1.350	1210	6000
1.370	1360	10250
1.390	1650	19857
1.395	1785	30942
1.400	2025	90500

As the refractive index of the solution increases, the efficiency of the device is decreased where *RI* = 1.400 is considered to be the upper limit of the proposed device. Due to limitations in manufacturing to tight tolerances, the effect of a fabrication tolerance of ±2% was studied. This investigation includes the effects of tolerance on the optimized parameters as well as the effects of nanowire misalignment. The results show a negligible variation with respect to the sensor optimum values of D = 0.2 µm and r_n = 0.5 µm and the misalignment from its mean position (varied by ±0.01 µm, ±0.03 µm, and ±0.05 µm). From this study, it is important to note that the sensor has been through multiple tolerance studies to attain the optimum sensing response. The achieved sensitivity of the designed sensor makes it a potential candidate in chemical and biological sensing for liquids and biofluids with a range of *RI* between 1.310 and 1.400. This includes glucose monitoring (*RI* = 1.360-1.390) [18], Immunoglobulin G and M monitoring (*RI* = 1.330-1.340) [19], blood component detection such as red blood cells (*RI* = 1.400), hemoglobin (*RI* = 1.380) [20], etc.

IV. CONCLUSION

In conclusion, we have reported a novel idea for the development of a DDC based SPR refractive index sensor with enhanced sensing response for a wide range of analytes with *RI* varying from 1.310-1.400. The sensing response of the sensor and the coupling characteristics of the DDC sensor have been numerically analyzed using the FEM technique. The achieved results exhibit a very high sensitivity between 10250 nm/RIU and 90500 nm/RIU for *RI* varying in range of 1.370-1.400. A sensitivity of 3150 nm/RIU can be obtained for *RI* = 1.310. Through this letter, we can conclude that the dual channel containing two AuNWs providing more light matter interaction compared to single channel with single AuNW, and hence resulting an extremely high sensitivity. This letter has addressed both the sensing configuration and the effects of fabrication tolerances on the sensor design. This study can be utilized to make the real-world application of the sensor more user-friendly as well as practically possible.

V. REFERENCES

[1] C. Viphavakit, S. O. Keeffe, M. Yang, S. Andersson-Engels, and E. Lewis, "Gold Enhanced Hemoglobin Interaction in a Fabry–Pérot Based Optical Fiber Sensor for Measurement of Blood Refractive Index," *J. Light. Technol.*, vol. 36, no. 4, pp. 1118–1124, Feb. 2018.

[2] A. Otto, "Excitation of nonradiative surface plasma waves in silver by the method of frustrated total reflection," *Zeitschrift für Phys. A Hadron. Nucl.*, vol. 216, no. 4, pp. 398–410, Aug. 1968.

[3] E. Kretschmann and H. Raether, "Notizen: Radiative Decay of Non Radiative Surface Plasmons Excited by Light," *Zeitschrift für Naturforsch. A*, vol. 23, no. 12, Jan. 1968.

[4] B. Liedberg, C. Nylander, and I. Lunström, "Surface plasmon resonance for gas detection and biosensing," *Sensors and Actuators*, vol. 4, pp. 299–304, Jan. 1983.

[5] X. Xie, J. Li, L.-P. Sun, X. Shen, L. Jin, and B. Guan, "A High-Sensitivity Current Sensor Utilizing CrNi Wire and Microfiber Coils," *Sensors*, vol. 14, no. 5, pp. 8423–8429, May 2014.

[6] H. Fu *et al.*, "A high sensitivity D-type surface plasmon resonance optical fiber refractive index sensor with graphene coated silver nano-columns," *Opt. Fiber Technol.*, vol. 48, pp. 34–39, Mar. 2019.

[7] D. Santos, A. Guerreiro, and J. M. Baptista, "Evaluation of Nanoplasmonic Optical Fiber Sensors Based on D-Type and Suspended Core Fibers with Metallic Nanowires," *Photonics*, vol. 6, no. 3, p. 100, Sep. 2019.

[8] A. K. Pathak, S.Ghosh, R.K.Gangwar, B.M.A.Rahman, and V. K. Singh, "Metal Nanowire Assisted Hollow Core Fiber Sensor for an Efficient Detection of Small Refractive Index Change of Measurand Liquid," *Plasmonics*, 2019.

[9] R. K. Gangwar, V. A. Amorim, and P. V. S. Marques, "High Performance Titanium Oxide Coated D-Shaped Optical Fiber Plasmonic Sensor," *IEEE Sens. J.*, vol. 19, no. 20, pp. 9244–9248, Oct. 2019.

[10] H. Kumar, U. Ramani, B. K. Singh, and P. C. Pandey, "Investigations on the Highly Sensitive Metal-Coated Broad Range D-Shaped Optical Fiber Refractive Index Sensor," *Plasmonics*, vol. 16, no. 6, pp. 1963–1971, Dec. 2021.

[11] R. A. Kadhim, A.-H. Nawar, A. K. K. Abdul, L. Yuan, and J. Wu, "Optical Fiber Refractive Index Sensor Based on the SPR Using a Multiple D-shaped Ag Nanowire," in *2020 IEEE SENSORS*, 2020, pp. 1–4.

[12] Nespereira, Coelho, and Rebordão, "A Refractive Index Sensor Based on a Fabry–Perot Interferometer Manufactured by NIR Laser Microdrilling and Electric Arc Fusion," *Photonics*, vol. 6, no. 4, p. 109, Oct. 2019.

[13] Y. S. Ong, W. Kam, S. W. Harun, R. Zakaria, and W. S. Mohammed, "Low-Cost Transducer Based On Surface Scattering Using Side-Polished D-Shaped Optical Fibers," *IEEE Photonics J.*, vol. 7, no. 5, pp. 1–10, Oct. 2015.

[14] X. Li, X. Guo, D. Wang, and L. Tong, "Propagation losses in gold nanowires," *Opt. Commun.*, vol. 323, pp. 119–122, Jul. 2014.

[15] H. W. Lee *et al.*, "Pressure-assisted melt-filling and optical characterization of Au nano-wires in microstructured fibers," *Opt. Express*, vol. 19, no. 13, p. 12180, Jun. 2011.

[16] A. Vial, A.-S. Grimault, D. Macías, D. Barchiesi, and M. L. de la Chapelle, "Improved analytical fit of gold dispersion: Application to the modeling of extinction spectra with a finite-difference time-domain method," *Phys. Rev. B*, vol. 71, no. 8, p. 085416, Feb. 2005.

[17] A. K. Pathak and C. Viphavakit, "VOC biomarker monitoring for diabetes through exhaled breath using Ag/P-TiO2 composite plasmonic sensor," *IEEE Sens. J.*, pp. 1–1, 2021.

[18] S. K. Chamoli, S. C. Singh, and C. Guo, "Design of Extremely Sensitive Refractive Index Sensors in Infrared for Blood Glucose Detection," *IEEE Sens. J.*, vol. 20, no. 9, pp. 4628–4634, May 2020.

[19] F. Chiavaioli, "Recent Development of Resonance-Based Optical Sensors and Biosensors," *Optics*, vol. 1, no. 3, pp. 255–258, Nov. 2020.

[20] V. Kaur and S. Singh, "Design approach of solid-core photonic crystal fiber sensor with sensing ring for blood component detection," *J. Nanophotonics*, vol. 13, no. 02, p. 1, May 2019.